Angewandte Communications

Catalyst Characterization

DOI: 10.1002/anie.201((will be filled in by the editorial staff))

Counting of oxygen defects vs. metal surface sites in methanol synthesis catalysts by different probe molecules**

*Matthias B. Fichtl, Julia Schumann, Igor Kasatkin, Nikolas C. Jacobsen, Malte Behrens, Robert Schlögl, Martin Muhler and Olaf Hinrichsen**

***Abstract**: Different surface sites of solid catalysts are usually quantified by dedicated chemisorption techniques from the adsorption capacity of probe molecules assuming they specifically react with unique sites. In case of methanol synthesis catalysts, the Cu surface area is one of the crucial parameters in catalyst design and was for over 25 years commonly determined using diluted N_2O. In order to disentangle the catalysts' components influence different model catalysts are prepared and characterized using N_2O, temperature programmed desorption of H_2 and kinetic experiments. It turns out that the presence of ZnO dramatically influences the N_2O measurements. This effect can be explained by the presence of oxygen defect sites which are generated at the Cu-ZnO interface and can be used to easily quantify the intensity of Cu-Zn interaction. It can be concluded that N_2O in fact probes the Cu surface plus the oxygen vacancies, whereas the exposed Cu surface area can be accurately determined by H_2.*

Methanol counts among the most important basic chemicals and represents an important C1 building block for industrial chemicals. It is commonly produced by hydrogenation of carbon monoxide or carbon dioxide. In the typically used low pressure process over $Cu/ZnO/Al_2O_3$ catalysts pressures ranging from 50 to 100 bar and temperatures of 483 to 563 K are employed.[1] Since methanol is a platform molecule and can in general be generated from sustainable hydrogen and CO_2 sources, it gathers rising attention as a renewable energy storage and carrier.[2]

Even today - 50 years after the commercial introduction of the $Cu/ZnO/Al_2O_3$ system - the nature of the active site(s) of methanol synthesis is still under heavy investigation and a vast amount of techniques is employed to elaborate the reaction mechanism and active centre of the methanol synthesis on copper.[3–6] This lack of understanding can be partially contributed to the strong interaction of the different catalyst components. Especially the role of zinc oxide is still under debate. The well known ZnO promotion of copper has been described by various mechanisms such as alloy material and structural support or a hydrogen reservoir providing adsorbed hydrogen to copper by spill-over.[7–10] Many promotional effects or the activity of pure ZnO in methanol synthesis have in some way been attributed to the reducibility of ZnO and the formation of oxygen vacancy sites and it was shown that the presence of oxygen defects is also a crucial factor for the methanol synthesis activity of pure ZnO.[5,11,12] In situ TEM and EXAFS studies have proven the formation of oxygen vacancy sites in ZnO depending on the reactive conditions over the catalyst. This behavior is specifically attributed to the Cu-ZnO interaction (SMSI effect) and the defect concentration is high enough to influence the copper particle morphology in model systems.[13–16] Recently Schott *et al.* reported about the aplanar distortion of thin ZnO layers on copper, leading to a systematically less strongly oxidized $Zn^{\delta+}$.[17] In real catalysts an amorphous overlayer of partially reduced ZnO_x influencing the adsorption properties of copper is found covering the copper particles after the activation procedure and the resulting catalyst characteristics have been extensively studied.[14,18] This can be seen as a precursor state to the partial formation of Cu-Zn surface alloys which in fact might be the driving force for the strong interaction.

The complexity of the typical surface termination of Cu nanoparticles in common $Cu/ZnO/Al_2O_3$ catalysts as formed after reduction is shown in the high-resolution TEM image in Figure 1. At the surface, a disordered 1-2 nm thick termination layer indicates the overgrowth of the Cu particle with disordered ZnO_x due to Cu-ZnO interaction under reducing conditions. It can be seen that the metal termination underneath this layer is very rough with many steps and missing atoms at the Cu-ZnO_x interface. These structural details suggest that the reactivity of such dynamic SMSI state in Cu/ZnO catalysts toward reactive probe molecules like N_2O might be more complex than simple monolayer chemisorption observed at well-defined pure Cu facets.[19]

[*] Matthias B. Fichtl, Olaf Hinrichsen
Catalysis Research Center and Chemistry Department, Technische Universität München, Lichtenbergstraße 4, D-85748 Garching b. München
Email: olaf.hinrichsen@ch.tum.de

Julia Schumann, Igor Kasatkin, Malte Behrens, Robert Schlögl
Department of Inorganic Chemistry, Fritz-Haber-Institut der Max-Planck-Gesellschaft, Faradayweg 4-6, D-14195 Berlin, Germany

Igor Kasatkin
Saint Petersburg State University, Research Centre for X-ray Diffraction Studies, 199155, Decabristov lane 16, St. Petersburg, Russia

Nikolas C. Jacobsen
Clariant Produkte (Deutschland) GmbH, BU Catalysts, Waldheimer Str. 13, D-83052 Bruckmühl, Germany

Martin Muhler
Ruhr-Universität Bochum, Fakultät für Chemie und Biochemie, Universitätsstrasse 150,D- 44780 Bochum, Germany

[**] Financial support was provided by the Bayerisches Wirtschaftsministerium (NW-0906-0002) and Clariant Produkte (Deutschland) GmbH. Matthias Fichtl gratefully acknowledges the support of the TUM Graduate School.

Supporting information for this article is available on the WWW under http://dx.doi.org/10.1002/anie.201xxxxxx.

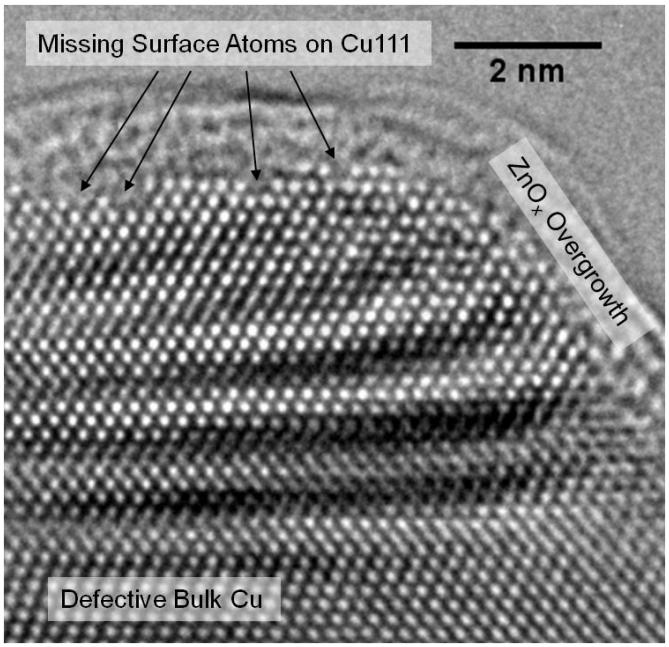

Figure 1. HRTEM image of the surface termination of the ZnO_x-overgrown Cu nanoparticles in the catalyst CMZ1. The contrast fluctuations seen in the bulk of the Cu particle are Moiré fringes arising due to partial overlapping with other particles.

From a structural point of view, it is not easy to decide if under working conditions the extent of ZnO reduction in such arrangement exceeds the observed $Zn^{\delta+}O_x$-covered Cu state and dynamically reaches a true surface alloy state. However, from a functional point of view, the difference of both models seems rather small as they have in common the existence of partially reduced and thus oxophilic $Zn^{\delta+}$ atoms in a close neighborhood to metallic Cu sites. These $Zn^{\delta+}$ sites are thought to act as adsorption sites for CO_2 and reaction intermediates like formate, while the hydrogen is likely supplied from the metallic Cu sites. A similar bi-functional mechanism was also proposed for methanol synthesis on Cu/ZrO_2 catalysts with CO_2 being activated on the surface of the zirconia promoter.[20] These CO_2 adsorption centers in Cu/ZrO_2 were modeled at the Cu-oxide interface, where in case of Cu/ZnO oxophilic $Zn^{\delta+}$ sites can be expected.[21] It has been shown that the contact to Cu can promote the formation of oxygen vacancies in ZnO.[22] Alternatively, functionally similar oxophilic Zn sites can be modeled by inserting metallic surface Zn atoms on Cu defect sites.[5]

The existence of such oxophilic sites due to ZnO reduction creates an inherent problem when looking at the "classic" characterization of methanol synthesis catalysts by reactive nitrous oxide frontal (N_2O-RFC) or pulse chromatography which has been performed for over 25 years in order to quantify the copper surface area.[23] Especially the assumption that N_2O specifically oxidizes the copper surface and ignores the partially reduced ZnO_x is questionable. This study investigates the influence of ZnO on the copper surface area measured by N_2O-RFC and hydrogen temperature programmed desorption (H_2-TPD) on different $Cu/ZnO/Al_2O_3$, Cu/ZnO, Cu/MgO and Cu/ZnO/MgO catalysts. It unravels the significant bias which is introduced by the oxidation of ZnO_x sites using H_2-TPD as a complementary characterization method which provides a very selective, sensitive and accurate way of describing the exposed copper surface area, i.e., the copper surface area not covered by ZnO_x species.[13]

In order to shed light on the interplay of exposed copper surface area, partially reduced zinc oxide and apparent N_2O-RFC area different model catalysts are prepared and characterized (supporting information I). With the purpose to elucidate the influence of the reducible ZnO component, also Al_2O_3 and MgO were studied as alternative, irreducible structural promoters. Table 1 gives an overview of the systems employed and their composition and BET surface areas. To study the effect of ZnO, a ZnO-impregnation was applied to the Cu/MgO system using different synthetic procedures.

Table 1. Compositions and BET surface areas of the catalysts used.

Sample	C/X[a, b]	S_{BET}[c]	Sample	C:X[a, b]	S_{BET}[c]
C	100/ -	15	CMZ1	79/16/5[d]	94
CA1	20:80	100	CMZ2	79/16/5[d]	90
CA2	87/13	70	CMZ3	67/29/4[d]	121
CM1	83/17	100	CZA1	43/49/8	78
CM2	70/30[d]	99	CZA2	58/26/16	74
ZA	-/84/16	78	CZA3	70/28/2	118

[a] Cu, Zn, Al, Mg = C, Z, A, M [b] molar, determined by ICP & XRF [c] calcined precursor, [$m^2\ g_{cat}^{-1}$] [d] nominal composition

After activation of the catalysts in a glass lined single-pass fixed-bed reactor (supporting information II) multiple H_2-TPD spectra are gathered at heating ramps of 4, 6 and 10 K min^{-1} (supporting information III). Next, the N_2O copper surface area is determined using the same catalyst at 308 K, 1 bar pressure using N_2O (1%) in He (supporting information IV). A mean copper surface density of $1.47 \cdot 10^{19}$ atoms per m^2 is used for converting the measured amount of copper into specific surface area. Activity measurements of the Zn-containing catalysts are performed after the H_2-TPD and N_2O-RFC measurements (supporting information II).

Correlating the hydrogen adsorption capacity and N_2-evolution during the N_2O-RFC - which should be proportional to the copper surface area according to both methods - reveals the heavy bias which is introduced by ZnO. This is shown in figure 2.

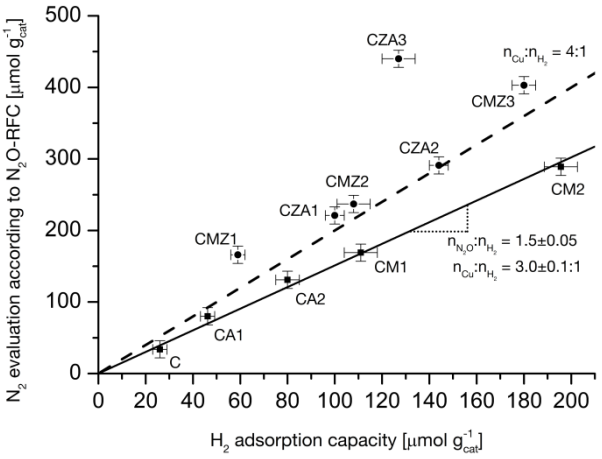

Figure 2. Correlation of the H_2-TPD and N_2O-RFC results.

The N_2O surface area of polycrystalline Cu agrees well with published data and the H_2-TPD area of the CA-systems matches with data published by Muhler et al. reasonably well.[5,24] Assuming the formal oxidation of the exposed copper surface on Zn-free samples by N_2O to Cu_2O, the Cu:H_2 ratio can be determined using equation 1 and the value of the decomposed N_2O per adsorbed H_2. This ratio n_{N_2O}:n_{H_2} is given by the slope of the solid line in figure 2.

$$\frac{Cu}{H_2} = 2 \cdot \frac{n_{N_2O}}{n_{H_2}} \quad \text{(eq 1)}$$

A Cu:H_2 ratio of 3.0±0.1:1 is obtained for the Zn-free materials. This experimental value mismatches the classically assumed 4:1 ratio, which is commonly deduced from UHV studies and described with a 0.5 monolayer (ML) coverage of copper.[25] However, the formation of a 2/3 ML coverage, which corresponds with the measured Cu:H_2 ratio, has been observed at higher H_2 exposure and theoretically studied in detail.[26–28] These findings are also in line with the formation of ordered 1/3 ML and 2/3 ML adsorption structures during dissociative hydrogen adsorption on other fcc type metals.[29]

The Cu/H_2 ratio is independent of the irreducible structural promotor and copper particle size. It also is in very good agreement with the BET surface area (3.1 $m^2g_{cat}^{-1}$) of the activated sample C. The fact that even the low-surface area polycrystalline copper sample C nicely matches the H_2-N_2O correlation underlines the high sensitivity and precision which is obtained using H_2-TPD. The Zn-containing catalysts show a non-linear behavior where the majority roughly follow a Cu:H_2 ratio of 4:1 (dashed line in figure 2). Generally, all Zn-containing systems yield a significant higher N_2O-copper surface area than would be expected from the corresponding H_2-TPD experiments. According to the concept of reduced ZnO_x on top of the particles, this can be explained by the overconsumption of N_2O by oxidizing partially reduced ZnO_x. Furthermore, the ZnO_x layer is not necessarily of a monolayer type and de-wetting of previously covered copper upon oxidation of ZnO_x has to be considered.

In case of H_2-TPD measurements it is reasonable to say that hydrogen desorption from ZnO_x species is not observed within the experimental window which is supported by the impregnation experiments (vide infra). In general the position of the H_2-TPD signal is sensitive to the adsorption enthalpy and in case of the examined copper catalysts well aligned with the desorption signal of metallic copper. The difference in measured N_2O-surface area and corresponding theoretical N_2O-surface area according to the H_2-TPD quantifies the amount of over-oxidation and hence oxophilic $Zn^{\delta+}$ sites in ZnO_x.

Although the ZA sample exhibits a comparable BET surface area, the H_2-TPD and N_2O-RFC measurements do not show any significant signals in the specified experimental window after activation. This supports the assumption that the high amount of measurable defect sites stems from the copper zinc interaction and is not introduced by the sheer presence of ZnO. The extent of this interaction will be promoted by an initially high inter-dispersion of both phases, which is a function of the catalyst preparation. Thus, a strict linear behavior in case of the Zn-containing catalysts is not expected *a priori*.

Recently Behrens et al. presented a systematic study about the homogeneous incorporation of the different metals in the methanol synthesis catalysts and presented a highly active system with an optimized incorporation of Al^{3+} in the ZnO phase, leading to a strong defect structure in ZnO_x.[30] The analogously to this publication prepared sample CZA3 nicely confirms this behavior, as the determined defect concentration is more than 100% higher than in the other conventional CZA and CMZ systems. Furthermore, the impregnation experiments of the CM samples support these findings. Normally a drop in metal surface area of the activated impregnated samples should be expected, as a ZnO_x overlayer is formed over the copper particles blocking them from chemisorption.[10] In case of the presented CMZ samples this is only true for the H_2-TPD measurements, whereas the N_2O-surface area even increases in comparison with the corresponding CM precursors. The results highlight the critical role of catalyst synthesis for the intensity of Cu-Zn interaction. The ZnO-impregnation of the calcined pre-catalyst (CM1 → CMZ1) leads to heavy blocking of half of the Cu surface area detected by the decrease in H_2 capacity and only a low degree of Cu-Zn interaction indicated by the little increase in N_2O capacity. Contrarily, if impregnation is done already on the co-precipitated catalyst precursor (CM1 → CMZ2 and CM2 → CMZ3), a much lower loss in Cu surface area and a substantial increase in N_2O capacity indicative for an intimate Cu-Zn interaction is observed.

The microstructure of the CZA catalysts was additionally characterized by TEM. As observed previously, the Cu particle shape can be described by a pseudo-spherical with an oxide matrix that spatially separates the individual nanoparticles. Based on a statistical Cu particle size evaluation, a theoretical maximal exposed Cu surface area can be calculated assuming that the particles were round and completely unsupported (Tab. 2). This value exceeds the probe gas derived surface areas in all cases, which is reasonable considering that a fraction of this hypothetical surface area must be present as interface to the stabilizing oxide matrix. A microstructural model of the catalyst in relation to the probe gas chemisorption capacities including the insensitivity of hydrogen toward Cu-ZnO interaction is discussed in the supporting information.

The specific activity evaluation of the Zn-promoted catalysts in figure 3 reveals that there is neither a direct correlation between the H_2-or N_2O-copper surface area and the catalyst activity nor between the catalyst activity and amount of oxophilic sites generated by ZnO. The latter one is estimated from the difference of the N_2O-RFC surface area and real copper surface which is calculated using the H_2-TPD data (see supporting information IV). According to the data, without optimization of the irreducible structural support (CZA3) this amount is almost constant independent of the preparation technique and Zn content. This implies again the Cu-Zn interaction as origin. Table 2 gives an overview of the determined specific surface areas.

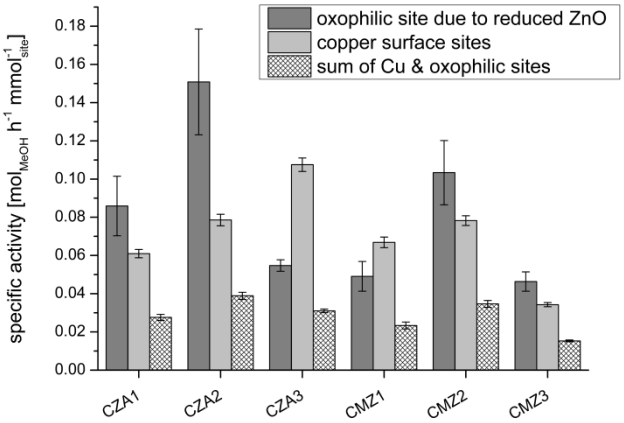

Figure 3. Specific activity of the different catalysts depending on the site type.

Table 2. Specific copper surface areas (SSA) and defect concentrations in SSA equivalents. (n.d. = not determined)

Sample	max. SSA_{TEM}[a]	$SSA_{H2\text{-}TPD}$[b]	$SSA_{N2O\text{-}RFC}$[b]	O defects[b]
CZA1	21.7	12.3	18.1	5.8
CZA2	27.9	17.7	23.8	6.1
CZA3	49.3	15.6	36.1	20.4
CMZ1	n.d.	7.1	13.6	6.5
CMZ2	n.d.	12.9	19.4	6.5
CMZ3	n.d.	22.1	33.0	11

[a] determined as described in the supporting information; [b] mass based on calcined precursor, [m^2 g_{cat}^{-1}]

The missing direct correlation between surface area and activity is not surprising and has been reported before, as the active site of the methanol synthesis is not considered to be metallic copper or the vacancy sites themselves, but a combination of multiple factors.[5,10,31] Interestingly with exception of CMZ3, there is a relationship between the N_2O-RFC surface area and the activity data, which suggests that the N_2O-RFC - despite the conceptual problem - can be used to characterize and evaluate many methanol synthesis catalysts. This trend has been reported in many literature reports, but was often misinterpreted as linear relationship between Cu surface area and activity to conclude structure-insensitivity of methanol synthesis on Cu/ZnO-based catalysts. In case of the highly active catalyst CZA3, it was shown that oxygen vacancies can in fact account for more than 50% of the N_2O-RFC capacity. This result shows that recent progress in catalyst development is not necessarily related to further increase in Cu surface area, but that great potential lies in the design of the Cu-Zn interaction. It furthermore strongly suggests that N_2O-derived surface areas should not be used to calculate TOFs of Cu/ZnO-based catalysts. While the N_2O capacity is an intrinsic and catalytically important property, it does not (only) represent the amount of metal surface sites, which can be better quantified by H_2 chemisorption.

In summary, we are able to show that the presence of ZnO introduces a heavy bias in the determination of copper surface area using N_2O-RFC whereas both the N_2O-RFC and H_2-TPD characterization methods lead to well matching results in absence of ZnO. Based on these measurements and recent findings about the nature of the Cu-ZnO interaction we propose, that an over 25 years established method for the characterization of the surface area of methanol synthesis catalysts does in fact not only describe the copper surface area, but also the oxygen defects which are present at the copper zinc interface. Although, the N_2O-RFC has often proved to be characteristic for the description of activity-structure relationships, it draws a misleading picture in terms of functional relationships in the catalysts and might lead to false assumptions for the mechanistic description and understanding. We are able to show that quantitative measurement of ZnO_x oxygen vacancies in methanol synthesis catalysts is possible by combining H_2-TPD and N_2O-RFC measurements. As both measurements can easily be done in situ in a fixed-bed reactor setup, this greatly enhances the possibility of systematic studies on methanol synthesis catalysts. With little adaption, these measurements can be extended to other important catalytic systems with a pronounced SMSI effect like many group VIII metals supported on reducible transition metal oxides.

Experimental Section

The catalysts C, CA1-2, CZA1-3, ZA, CM1-2 and CMZ1-3 are produced via co-precipitation following literature recipes (see supporting information I). The catalyst activity and the copper surface area according to H_2-TPD and nitrous oxide reactive frontal chromatography (N_2O-RFC) are determined in a glass lined single-pass fixed-bed reactor described in the supporting information II. A detailed description of the procedures for the activity tests, N_2O-RFC and H_2-TPD measurements is given in the supporting information II, III and IV.

Received: ((will be filled in by the editorial staff))
Published online on ((will be filled in by the editorial staff))

Keywords: Catalyst-support interaction • Copper • Heterogeneous catalysis • Methanol • Oxygen defect sites

[1] R. Malhotra, *Fossil Energy: Selected Entries from the Encyclopedia of Sustainability Science and Technology*, Springer, New York, **2012**.
[2] G. A. Olah, *Angew. Chem. Int. Ed.* **2013**, *52*, 104–107.
[3] L. C. Grabow, M. Mavrikakis, *ACS Catal.* **2011**, *1*, 365–384.
[4] T. Askgaard, *J. Catal.* **1995**, *156*, 229–242.
[5] M. Behrens, F. Studt, I. Kasatkin, S. Kühl, M. Hävecker, F. Abild-Pedersen, S. Zander, F. Girgsdies, P. Kurr, B.-L. Kniep, et al., *Science* **2012**, *336*, 893–897.
[6] C. V. Ovesen, B. S. Clausen, J. Schiøtz, P. Stoltze, H. Topsøe, J. K. Nørskov, *J. Catal.* **1997**, *168*, 133–142.
[7] M. S. Spencer, *Top. Catal.* **1999**, *8*, 259–266.
[8] T. Fujitani, J. Nakamura, *Catal. Lett.* **1998**, *56*, 119–124.
[9] R. N. d' Alnoncourt, X. Xia, J. Strunk, E. Löffler, O. Hinrichsen, M. Muhler, *Phys. Chem. Chem. Phys.* **2006**, *8*, 1525–1538.
[10] S. Zander, E. L. Kunkes, M. E. Schuster, J. Schumann, G. Weinberg, D. Teschner, N. Jacobsen, R. Schlögl, M. Behrens, *Angew. Chem. Int. Ed.* **2013**, *52*, 6536–6540.
[11] S. Polarz, J. Strunk, V. Ischenko, M. W. E. van den Berg, O. Hinrichsen, M. Muhler, M. Driess, *Angew. Chem. Int. Ed* **2006**, *45*, 2965–2969.
[12] M. Kurtz, J. Strunk, O. Hinrichsen, M. Muhler, K. Fink, B. Meyer, C. Wöll, *Angew. Chem. Int. Ed.* **2005**, *44*, 2790–2794.
[13] H. Wilmer, O. Hinrichsen, *Catal. Lett.* **2002**, *82*, 117–122.
[14] J.-D. Grunwaldt, A. Molenbroek, N.-Y. Topsøe, H. Topsøe, B. S. Clausen, *J. Catal.* **2000**, *194*, 452–460.
[15] P. L. Hansen, J. B. Wagner, S. Helveg, J. R. Rostrup-Nielsen, B. S. Clausen, H. Topsøe, *Science* **2002**, *295*, 2053–2055.
[16] P. C. K. Vesborg, I. Chorkendorff, I. Knudsen, O. Balmes, J. Nerlov, A. M. Molenbroek, B. S. Clausen, S. Helveg, *J. Catal.* **2009**, *262*, 65–72.
[17] V. Schott, H. Oberhofer, A. Birkner, M. Xu, Y. Wang, M. Muhler, K. Reuter, C. Wöll, *Angew. Chem. Int. Ed.* **2013**, *52*, 11925–11929.
[18] T. Fujitani, J. Nakamura, *Applied Catalysis A: General* **2000**, *191*, 111–129.
[19] L. Martínez-Suárez, J. Frenzel, D. Marx, B. Meyer, *Phys. Rev. Lett.* **2013**, *110*, 086108.
[20] I. A. Fisher, H. C. Woo, A. T. Bell, *Catalysis Letters* **1997**, *44*, 11–17.
[21] Q.-L. Tang, Q.-J. Hong, Z.-P. Liu, *Journal of Catalysis* **2009**, *263*, 114–122.
[22] J. Xiao, T. Frauenheim, *J. Phys. Chem. Lett.* **2012**, *3*, 2638–2642.
[23] G. C. Chinchen, C. M. Hay, H. D. Vandervell, K. C. Waugh, *Journal of Catalysis* **1987**, *103*, 79–86.
[24] M. Muhler, L. P. Nielsen, E. Törnqvist, B. S. Clausen, H. Topsøe, *Catal. Lett.* **1992**, *14*, 241–249.
[25] G. Anger, A. Winkler, K. D. Rendulic, *Surface Science* **1989**, *220*, 1–17.
[26] G. Lee, D. B. Poker, D. M. Zehner, E. W. Plummer, *Surface Science* **1996**, *357–358*, 717–720.
[27] M. F. Luo, G. R. Hu, M. H. Lee, *Surface Science* **2007**, *601*, 1461–1466.
[28] E. M. Mccash, S. F. Parker, J. Pritchard, M. A. Chesters, *Surface Science* **1989**, *215*, 363–377.
[29] T. Mitsui, M. K. Rose, E. Fomin, D. F. Ogletree, M. Salmeron, *Nature* **2003**, *422*, 705–707.
[30] M. Behrens, S. Zander, P. Kurr, N. Jacobsen, J. Senker, G. Koch, T. Ressler, R. W. Fischer, R. Schlögl, *J. Am. Chem. Soc.* **2013**, *135*, 6061–6068.
[31] O. Martin, J. Pérez-Ramírez, *Catal. Sci. Technol.* **2013**, *3*, 3343–3352.

Entry for the Table of Contents (Please choose one layout)

Layout 1:

Catalyst Characterization

Matthias B. Fichtl, Julia Schumann, Igor Kasatkin, Nikolas C. Jacobsen, Malte Behrens, Robert Schlögl, Martin Muhler and Olaf Hinrichsen * _____
Page – Page

Counting of oxygen defects vs. metal surface sites in methanol synthesis catalysts by different probe molecules

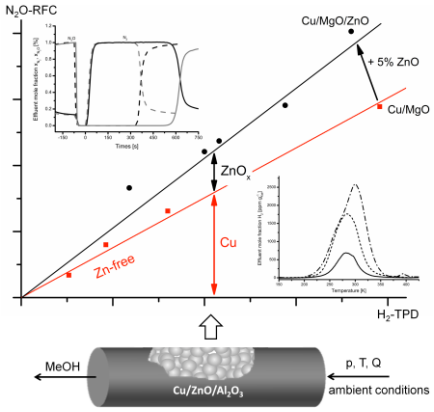

A combination of N_2O reactive frontal chromatography and H_2 temperature programmed desorption is used to analyze the interplay of copper and zinc oxide in methanol synthesis catalysts. This method provides an easy *in situ* approach to quantify the direct copper - zinc interaction (SMSI effect) and offers an important possibility to rational catalyst design also for other supported metal catalysts.

Layout 2:

Catch Phrase

Author(s), Corresponding Author(s)*
_____ **Page – Page**

Title Text

((TOC Graphic))

Text for Table of Contents, max. 450 characters.

Supporting Information

Table of content:

I) Catalyst preparation and characterization

The catalysts C, CA2, ZA, CZA1 and CZA2 are produced by coprecipitation of the metal nitrates at a constant pH of 7 and temperature of 333 K following the recipe presented in ref. [1]. CZA3 is a reproduction of the catalyst described in previous work and detailed characterization data can be found therein and in a forthcoming publication.[2] The synthesis procedure is also based on co-precipitation using the concept of the industrial catalyst, which has been recently reviewed in detail elsewhere.[3] In brief, aqueous nitrate solutions of the metals in a Cu:Zn = 70:30 ratio with additional 3 mol% of Al were co-precipitated at a constant pH of 6.5 using sodium carbonate as precipitating agent. The co-precipitate was aged in the mother liquor at 338 K to crystallize a substituted malachite precursor phase, $(Cu,Zn)_2(OH)_2CO_3$ (M = Zn). The precursor was calcined in air at 603 K to yield a CuO/ZnO:Al pre-catalyst with an intimate mixture of the oxides.

The Cu/MgO catalysts labeled CM were produced accordingly, but at a constant pH of 9 to completely precipitate the Mg^{2+} ions. The Cu-to-Mg ratio was 80:20 (CM1) or 70:30 (CM2), allowing co-precipitation of a phase-pure Mg-substituted malachite precursor, $(Cu,Mg)(OH)_2CO_3$, and subsequent transformation into a uniform material upon calcination and reduction. The follow-up impregnation of the CM catalysts with Zn-citrate to yield CMZ catalyst with a ZnO loading of 5 wt.% was done either on the malachite-like precursors of CM1 and CM2 (CMZ2 and CMZ3) or on the calcined CuO/MgO pre-catalyst of CM1 (CMZ1). In the latter case the catalyst was recalcined at 563 K. The resulting nominal molar ratios of the catalysts are given in Table S1. The catalysts CM1 and CMZ1 are identical or reproductions of the catalysts already described in previous work.[4] The Cu/Al_2O_3 catalyst CA1 was co-precipitated from a Cu:Al = 20:80 solution at pH8, washed and calcined at 603 K.

Table S1 provides an overview of selected samples used in this study and reports the internal FHI sample database numbers that should be used in future correspondence to facilitate communication.

Table S1. Sample overview and database numbers of selected catalysts.

Label	Metal composition (nominal, molar)	Precursor	Calcined	Remark
CZA3	$Cu/ZnO/Al_2O_3$ (70/28/2)	14328	15018	Reproduction of ref. [2]
CM1	Cu/MgO (80:20)	9278	15882	Precursor identical to ref. [4], calcination reproduced
CM2	Cu/MgO (70:30)	15316	15883	Analogous to CM1 besides composition
CMZ1	Cu/MgO/ZnO (79:16:5)	9278	13537	Precursor identical to ref. [4], impregnation reproduced on calcined catalyst
CMZ2	Cu/MgO/ZnO (79:16:5)	9278	13192	Precursor identical to ref. [4], impregnation was done on co-precipitated precursor
CMZ3	Cu/MgO/ZnO (67:29:4)	15316	16180	Precursor identical to CM2, impregnation was done on co-precipitated precursor
CA1	Cu/Al_2O_3 (20:80)	13560	16090	-

The metal content of the calcined C, CA2, ZA and CZA1-2 precursors is analyzed by ICP-OES (SpectroFlame FTMOA81A, Spectro Analytical Instruments). Using this method, the samples are also checked for the absence of sodium and potassium impurities. Prior to the analysis, the samples are dissolved in boiling aqua regia, inspissated and diluted with 1M HNO_3. Those samples listed in Tab. S1 have been investigated by X-ray fluorescence (XRF) using a Bruker S4 Pioneer X-ray spectrometer.

Nitrogen physisorption of the calcined precursors is measured at 78 K in a NOVA 4000e Surface Area & Pore Size Analyzer (Quantachrome Instruments). Prior to analysis, all samples are outgassed under vacuum at 523 K for 3 h. For analysis of the BET surface area ten evenly spaced points in the pressure region from 0.05 to 0.3 bar are used.

For high resolution TEM investigation shown in Figure 1 of the main article and Figure S6c,d, a FEI Titan Cs 80-300 microscope operated at 300 kV, equipped with a FEG, Gatan Tridiem Filter was used. Spherical aberrations were corrected by use of the CEOS C_s-corrector reaching an information limit of 0.8 Å. The particle size evaluation leading to the TEM-based Cu surface area estimations given in Table 2 of the main article was based on images such as shown in Figure S1, which were taken on A Philips CM200FEG microscope operated at 200 kV. The high-resolution image shown in Figure S6a was taken on the same machine and processed to obtain the power spectra which were used to measure inter-planar distances and angles for phase identification. For all measurements the reduced samples (at 250°C for 30 min in 5% H_2/Ar) were transferred via a glovebox to the microscope using a vacuum transfer holder to exclude the contact to air.

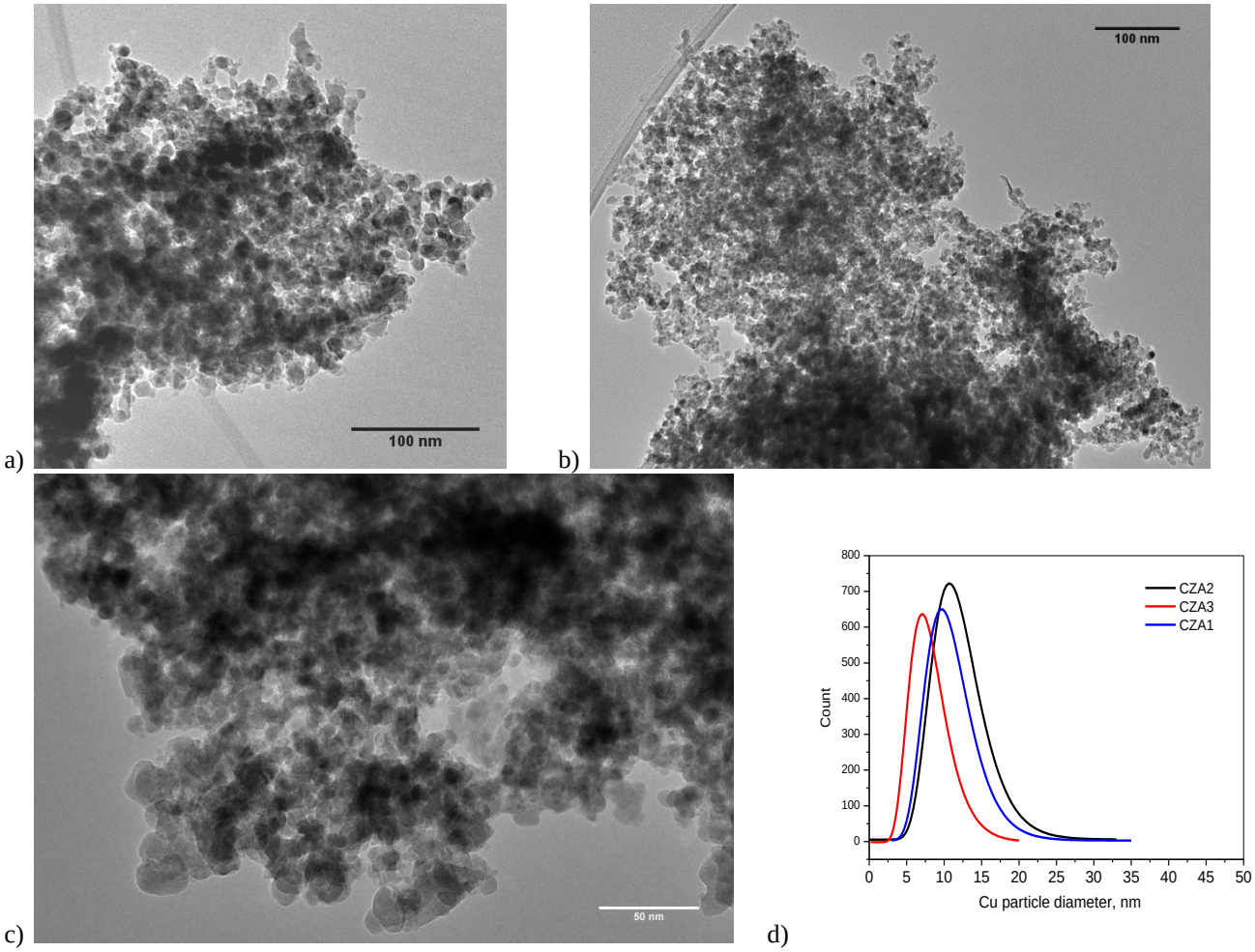

Figure S1. Representative TEM images of the catalysts CZA1 (a), CZA2 (b) and CZA3 (c) taken at moderate magnification for a statistical evaluation of the Cu particle sieze. Based on counting of thousands of Cu particles, the particle size distributions were determined. The log-normal fits to the obtained size histograms are shown in (d).

Based on a statistical evaluation of the Cu particle sizes of several images such as shown in Figure S1a-c, the particle size distribution (Fig. S1d) and the average volume weighted Cu particle sizes for CZA1, CZA2 and CZA3 were determined as 11.9, 13.4 and 8.9 nm, respectively. These values have been used to calculate the hypothetical maximal Cu surface area given in Table 2 of the main article based on the elemental compositions and assuming a spherical shape and bulk density of copper.

II) Experimental setup and activation procedure

The catalyst activity and the copper surface area according to H_2-TPD and nitrous oxide reactive frontal chromatography (N_2O-RFC) are determined in a glass lined single-pass fixed-bed reactor (internal diameter 4.5 mm) with internal thermocouple, an upstream gas mixing unit and a prior to every experiment calibrated mass spectrometer (Pfeiffer Vacuum OmniStar GSD 301 O) for time resolved in-situ analysis, as well as an Agilent 7820A gas chromatograph equipped with two thermal conductivity detectors, a packed Porapack-N column (Sigma Aldrich) for the quantification of CH_4, CO_2, H_2O, CH_2O, CH_3OH and a packed Molsieve 5 Å column (Sigma Aldrich) for the quantification of Ar, N_2, CH_4 and CO. The setup can be pressurized up to 28 bar and operated in a temperature range from 77 K up to 773 K. During the catalyst activation, N_2O-RFC and activity measurements each catalyst is treated with the same premixed gases of the following compositions and purities: 2% H_2 (99.9999%)/He (99.99999), 1% N_2O (99.9990%)/He(99.9999%), 13.5% CO (99.997%)/3.5% CO_2 (99.9995%)/9.5% N_2 (99.9999)/73.5% H_2 (99.9999%). All other measurements are conducted using single high purity gases: H_2, He, N_2 99.9999%. In order to remove traces of sulfur and carbonyls from the synthesis gas stream, a guard reactor is employed.

In a typical measurement 75 mg up to 150 mg catalyst (according to the expected amount of surface area) of the 250-355 µm sieve fraction and 500 mg purified silicon carbide of the same sieve fraction are heated up at atmospheric pressure for 15 hours in 2.0% H_2 in He raising the temperature from 300 to 448 K at 1 K min^{-1}, then in pure H_2 raising the temperature from 448 K to 513 K at 1 K min^{-1} and holding for 30 minutes. Under these conditions no brass formation in the catalyst bulk phase takes place.[5] In all cases a specific flow rate of 0.2 sccm g_{cat}^{-1} is used.

The activity studies are performed after the H_2-TPD and N_2O-RFC measurements at 24 bar in synthesis gas (13.5% CO, 3.5% CO_2, 9.5% N_2, 3.5% H_2). The temperature ranges from 453 K to 523 K. Prior to the study, the catalysts are reactivated for 60 minutes at 448 K in 2% H_2/He. All conversions were checked to be lower than 10% of the corresponding equilibrium conversion, the selectivity is in all cases beyond 99% and the mass balances are within 3% relative accuracy. In case of the most active sample CZA3, the formation of hotspots has been thoroughly checked to be absent by varying the dilution with SiC. Here, also the absence of intraparticle diffusion limitation was checked using different particle sieve fractions. The results are given in figure S4.

III) Hydrogen Temperature Programmed Desorption (H_2-TPD)

After the activation procedure, the catalyst is cooled down in helium to 235 K and pressurized for 30 minutes with 24 bar H_2. Variation of the adsorption pressure and adsorption time showed, that a full hydrogen coverage of copper can be achieved using these conditions. After the adsorption period the catalyst is rapidly cooled down to 77 K, depressurized to 1 bar and flushed with He for another 30 minutes until the H_2 baseline in the mass spectrometer is stable. The H_2-TPD experiment is conducted at 1 bar using a He flow rate of 100 sccm and heating rates β of 4, 6 and 10 K min^{-1}. It has been shown that under these conditions transport limitations are absent.[6] The amount of hydrogen is calculated using the full area under the desorption peak. In this context, signals above 375 K are ignored.

Exemplary results of the N_2O-RFC and H_2-TPD measurements are given in figure S2 and give an impression of the high data quality available for the detailed description of the catalyst surface. Even for the - compared to the other catalysts - low dispersion of pure copper a clean and distinct H_2-TPD signal is visible. To our knowledge, this is the first time that a clean and fully covered H_2-TPD of polycrystalline copper is presented under atmospheric conditions. The obtained H_2-TPD peak temperatures (heating rate β = 6 K min^{-1}: C & CA systems 283±2 K, CZA systems 300±2 K) are in good agreement with published data.[7,8] Whereas in the C, CA and CM samples the desorption curve is perfectly symmetric, in the case of all CZA and CMZ catalysts a typical asymmetric curve is visible, which has been attributed to the morphologic structure of the copper particles.[9,10] However, it should be noted that the MgO supported samples show no shift of the H_2-desorption maximum after impregnation with ZnO but resemble the same shape and peak values as CZA samples. Careful reproduction of the experiments with fresh catalyst were performed with C, CA2 and CZA3, resulting in a maximum error margin of 5% for the H_2 area and ±2 K for the peak temperature. Temperature effects due to the position of the catalyst bed in the reactor have not been observed. With exception of the pure copper sample C no sintering tendencies are observed. The H_2 amount is also independent from the heating rate β. For every catalyst, the reported error bars are a result of at least three measurements, in case of the copper sample C three measurements each with fresh catalyst are employed. In all cases, the activated samples show no or very small traces of water contamination (signals at T > 375 K)[11] or other desorption signals within the given temperature range. Also no signal can be found in the given temperature range reproducing the experiments with pure SiC.

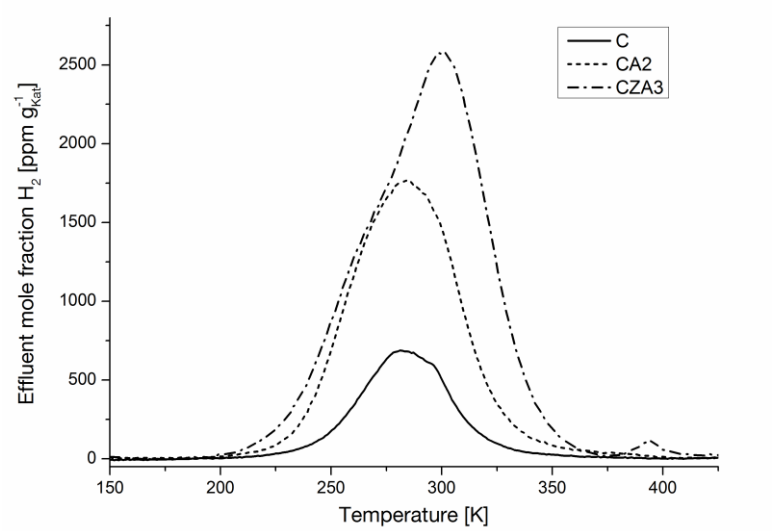

Figure S2. Exemplary H_2-TPD study on activated methanol synthesis catalysts. Measurement conditions: Q = 100 sccm, m_{cat} = 100 mg (based on calcined precursor), β = 6 K min^{-1}

IV) Nitrous Oxide-Reactive Frontal Chromatography

The N_2O copper surface area is determined using the activated catalyst sample after the H_2-TPD treatment at 308 K, 1 bar pressure and a flow rate setpoint of 7.5 sccm N_2O (1%) in He. The actual flow rate is determined prior and after the measurement with an automatic flow meter (BIOS Definer 220). At the chosen temperature, no significant bulk oxidation of copper is present and the N_2O decomposes according to theory quantitatively on the copper surface following the reaction:[12]

$$N_2O + 2\,Cu_{surface} \rightarrow Cu_2O + N_2$$

Holding the reactor under helium, the remaining setup is flushed with N_2O/He and after switching the reactor to 1% N_2O/He a breakthrough curve in the reactor effluent stream is measured using the calibrated mass spectrometer. The amount of copper surface atoms is calculated from the catalyst mass, exact flow rate and nitrogen area until the N_2O breakthrough. The specific Cu metal surface area is determined by using a value of $1.47 \cdot 10^{19}$ atoms per m^2 for the mean Cu surface atom density. The latter one is the arithmetic mean value of the low index planes Cu (111), Cu (110), Cu(100). As the subsurface oxidation cannot be completely avoided, the intersection between the falling N_2 signal and rising N_2O signal at the breakthrough point is used as a limit for the integration of the N_2 signal and a conservative error margin of 1 $m^2\ g_{cat}^{-1}$ (12 µmol $N_2O\ g_{cat}^{-1}$) is assumed, which is higher than the actual measured error when reproducing the experiments. An exemplary N_2O-RFC curve is given in figure S3 and the results are given in figure S4. The amount of oxophilic sites generated by the presence of ZnO is calculated from the difference of theoretical N_2O-adsorption capacity according to the copper surface determined via H_2-TPD and experimentally measured N_2O-adsorption capacity:

$$n_{defects} = n_{N_2O,experiment} - \frac{1}{2} n_{Cu,surface} = n_{N_2O,experiment} - \frac{3}{2} n_{H_2\text{-}TPD}$$

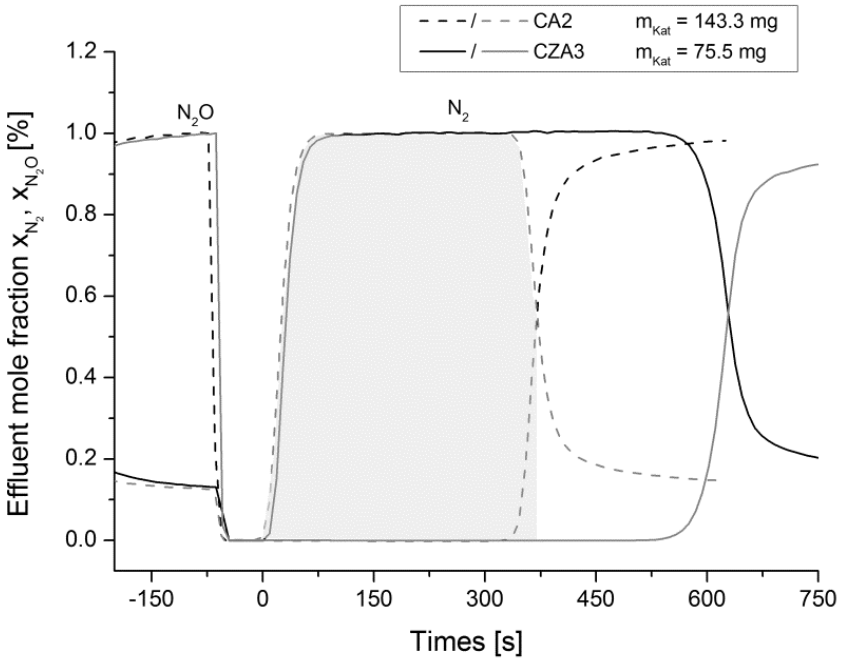

Figure S3. Exemplary N_2O-RFC curves of two catalysts. In case of CA2, the area used to determine the amount of produced N_2 is shaded gray. Experimental conditions: T = 308 K, p = 1 bar, Q = 7.5 sccm.

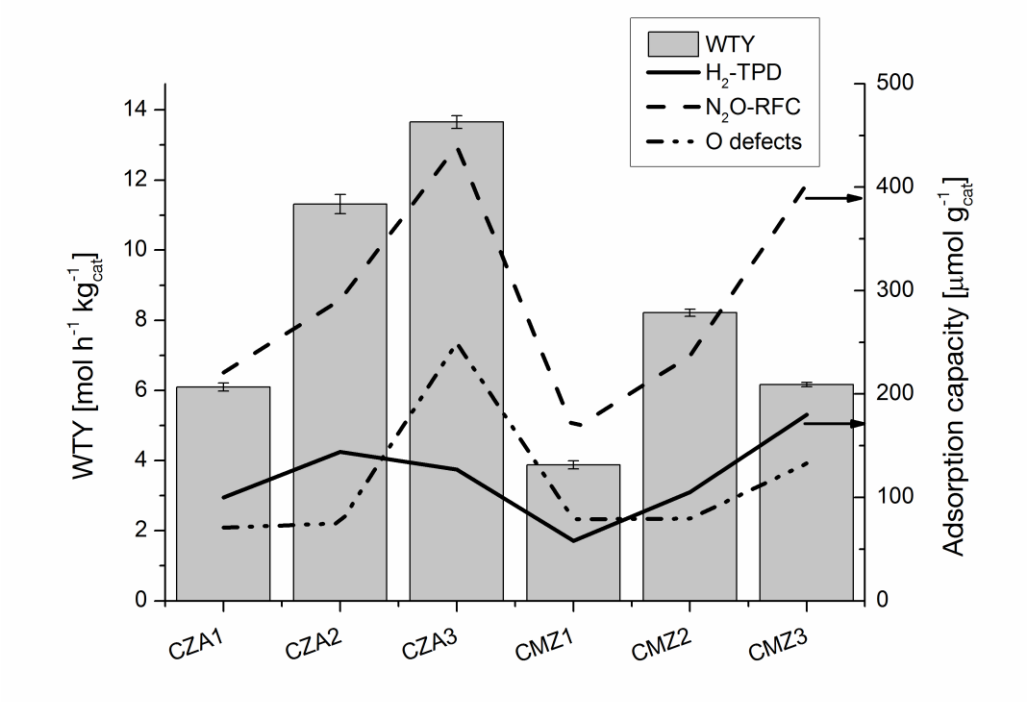

Figure S4. Graphical representation of the activity measurements and determined adsorption capacities according to N_2O-RFC, H_2-TPD and corresponding amount of oxophilic sites generated by the presence of ZnO.

V) Model For The Microstructure of Common Cu/ZnO/(Al_2O_3) Methanol Synthesis Catalysts

Figure S5 shows a comparison of the expected "specific Cu surface areas" of the CZA catalysts in m^2g^{-1}, that is obtained if the N_2O chemisorption capacity is conventionally evaluated as probing the metallic surface only. The values are compared to the hypothetical maximal Cu surface area as determined by TEM and to the real Cu surface area as determined by H_2 chemisorption. As described in the main text in detail, the discrepancy of N_2O and H_2 Cu surface areas in all ZnO-containing catalysts can be explained with the contribution of SMSI-induced defect sites of ZnO. While it seems clear that the "extra N_2O" is consumed on (partially) reduced Zn sites, we here make an attempt to relate these surface area differences with the microstructure of the Cu/ZnO/Al_2O_3 catalyst as shown in the TEM images in Figures 1, S1 and S6.

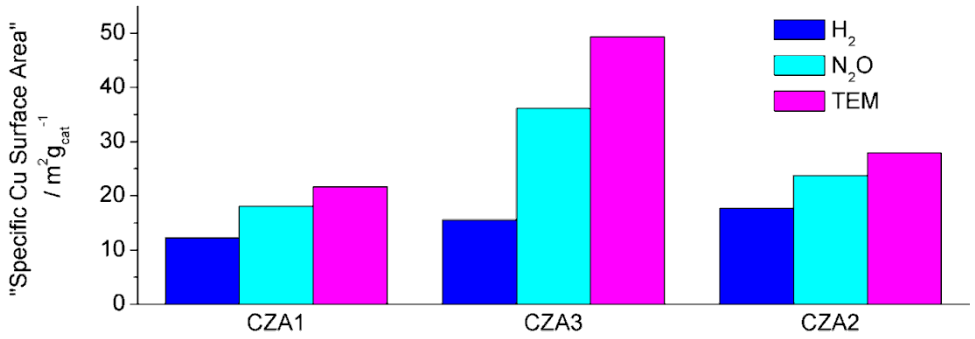

Figure S5. Comparison of the probe gas capacities of the CZA catalysts in this study if interpreted as specific Cu surface areas with the hypothetical maximal Cu surface area determined by TEM investigations shown in Figure S1.

Images of the microstructure of methanol synthesis catalysts are shown in Figures 1 (main text) and S6a-c as HRTEM and schematic representation. Typically, a disordered ZnO_x layer of 1-2 nm is found at the surface of the Cu particles after reduction. In rare cases, the ZnO_x overgrowth shows atomic ordering like in Figure S6c or stabilizes the atomically flat low-energy (111) facets of Cu and show a smaller down to the monolayer thickness, like the one in Figure S6d on the left side of the particle.

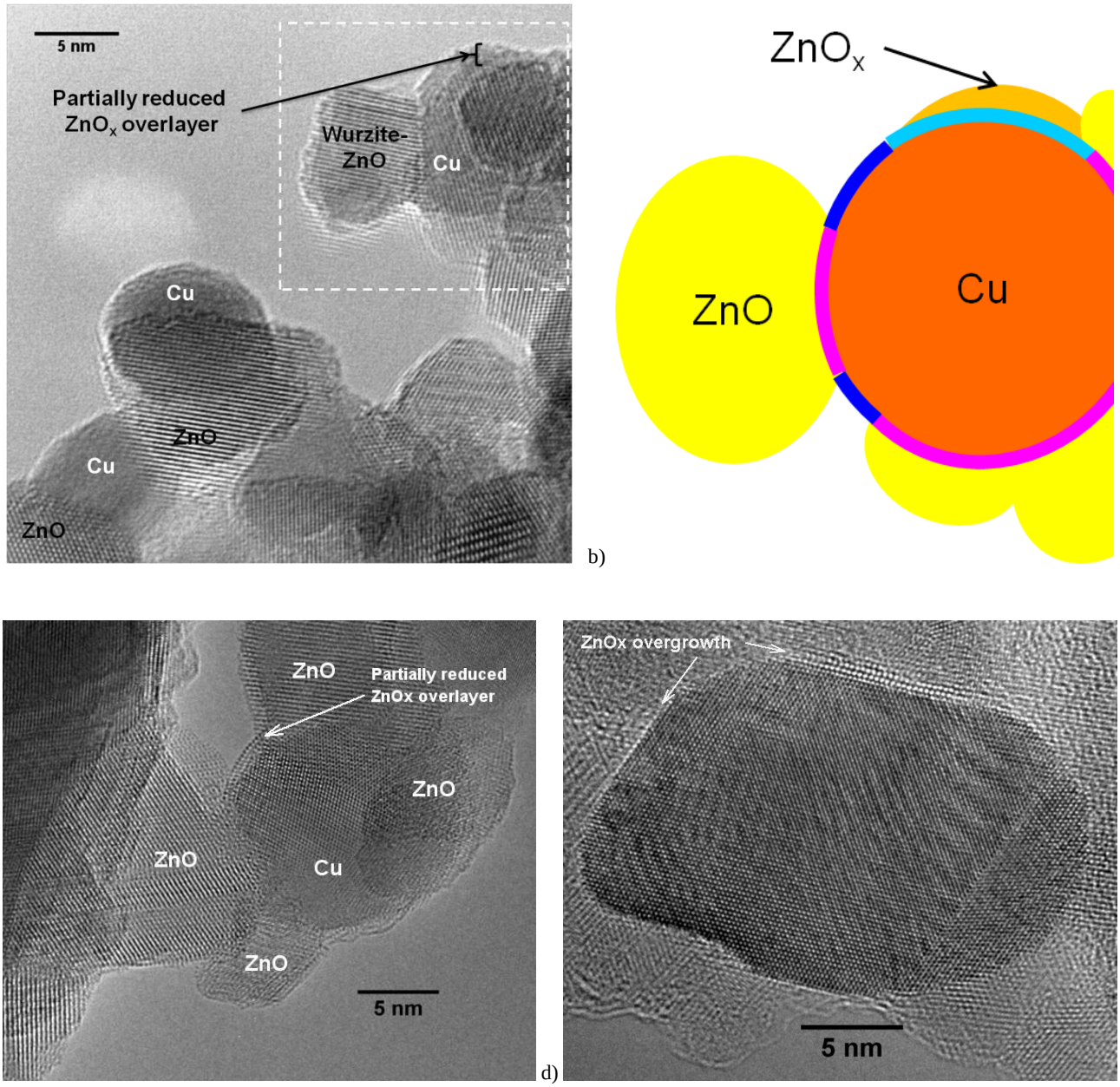

Figure S6. Representative HRTEM image of the catalysts CZA1 (a,c,d) and a schematic representation of a cross-section of the area in the dashed box (b). The color code refers to a proposed microstructural interpretation of the measured probe gas capacities shown in Fig. S5 and is explained in the text,

We assume that three types of Cu surfaces/interfaces exist: (i) a fraction present as interface to Wurzite-type ZnO particles that act as physical support of the Cu particles, (ii) a fraction that is covered by ZnO_x-overgrowth as shown in Figure 1 of the main article and thus involved in Cu-ZnO interaction; and (iii) a fraction that is uncovered and directly exposed to the gas phase. A suggestion of the microstructural arrangement of these types of surfaces in the catalysts is indicated in Figure S6b using pink color for type (i), light blue to type (ii) and dark blue for type (iii).

According to this simplified interpretation, the difference between TEM and N_2O surface areas can be seen as an estimate of the contact area between Cu and Wurzite-type ZnO, which are inaccessible for probe molecules and guarantees structural integrity to the catalysts (type (i)). The N_2O surface area would be the sum of type (ii) and type (iii), i.e. the difference between N_2O and H_2 surface areas is a measure for the degree of Cu-ZnO interaction, leading to partial reduction of ZnO and formation of ZnO_x-overgrowth. Finally type (iii) is directly measured by H_2 chemisorption. According to the quantification shown in Figure S5, this interpretation seems reasonable. However, other models involving, e.g., surface alloy formation or dynamic de-wetting of Cu are possible as well. In particular, the reactivity of the ZnO_x-overlayer toward O and H atoms is not clear and needs further investigation. Independent of these structural details, the better correlation of the N_2O-derived chemisorption capacity with the methanol synthesis activity within this catalyst series (sum of metallic Cu and oxophilic $Zn^{\delta+}$ sites) compared to the H_2-derived capacity (only Cu sites) or the difference of both (only $Zn^{\delta+}$ sites) supports the idea of a bi-functional active site for methanol synthesis.

References

[1] E. B. M. Doesburg, R. H. Höppener, B. de Koning, X. Xiaoding, J. J. F. Scholten, in *Preparation of Catalysts IV Scientific Bases for the Preparation of Heterogeneous Catalysts: Proceedings of the Fourth International Symposium; Louvain-La-Neuve, September 1-4, 1986* (Ed.: B. Delmon, F. Grange, P.A. Jacobs, G. Ponclet), Elsevier, Amsterdam, **1987**, pp. 767–780.

[2] M. Behrens, S. Zander, P. Kurr, N. Jacobsen, J. Senker, G. Koch, T. Ressler, R. W. Fischer, R. Schlögl, *J. Am. Chem. Soc.* **2013**, *135*, 6061–6068.

[3] M. Behrens, R. Schlögl, *Z. anorg. allg. Chem.* **2013**, *639*, 2683–2695.

[4] S. Zander, E. L. Kunkes, M. E. Schuster, J. Schumann, G. Weinberg, D. Teschner, N. Jacobsen, R. Schlögl, M. Behrens, *Angew. Chem. Int. Ed.* **2013**, *52*, 6536–6540.

[5] T. Kandemir, D. Wallacher, T. Hansen, K.-D. Liss, R. Naumann d'Alnoncourt, R. Schlögl, M. Behrens, *Nuclear Instruments and Methods in Physics Research Section A: Accelerators, Spectrometers, Detectors and Associated Equipment* **2012**, *673*, 51–55.

[6] M. Peter, J. Fendt, H. Wilmer, O. Hinrichsen, *Catal. Lett.* **2012**, *142*, 547–556.

[7] T. Genger, O. Hinrichsen, M. Muhler, *Catal. Lett.* **1999**, *59*, 137–141.

[8] H. Wilmer, T. Genger, O. Hinrichsen, *J. Catal.* **2003**, *215*, 188–198.

[9] M. Peter, J. Fendt, S. Pleintinger, O. Hinrichsen, *Catal. Sci. Tech.* **2012**, *2*, 2249.

[10] H. Wilmer, O. Hinrichsen, *Catal. Lett.* **2002**, *82*, 117–122.

[11] O. Hinrichsen, T. Genger, M. Muhler, in *Studies in Surface Science and Catalysis* (Eds.: A. Corma, F.V. Melo, S. Mendioroz, J.L.G. Fierro), Elsevier, **2000**, pp. 3825–3830.

[12] O. Hinrichsen, T. Genger, M. Muhler, *Chem. Eng. Technol.* **2000**, *23*, 956–959.